INSTITUTE OF PHYSICS PUBLISHING METROLOGIA
Metrologia **41** (2004) 161–166 PII: S0026-1394(04)75578-4

# Spatial and angular responsivity measurements of photoconductive HgCdTe LWIR radiometers

**H Gong[1,2], L M Hanssen[1] and G P Eppeldauer[1]**

[1] Optical Techonolgy Division, National Institute of Technology, Gaithersburg, MD 20899, USA
[2] State Key Laboratories of Transducer Technology, Shanghai Institute of Technical Physics, Chinese Academy of Sciences, Shanghai, People's Republic of China

Received 12 August 2002
Published 7 April 2004
Online at stacks.iop.org/Met/41/161
DOI: 10.1088/0026-1394/41/3/008

**Abstract**
Several newly developed large area photoconductive (PC) mercury cadmium telluride (HgCdTe) radiometers have been tested for spatial and angular responsivity for the purpose of determining what mode of operation (or radiometric quantity) could provide the lowest measurement uncertainty. An infrared (IR) test facility has been developed for the characterization of long wavelength IR (LWIR) detectors and radiometers for spatial response uniformity in power measurement mode and angular responsivity in both power and irradiance measurement modes. We have measured 34% to 53% spatial response non-uniformities and 1.5% to 10.5% changes in angular power reponsivity at different beam positions within the $f/4$ field-of-view (FOV) of the PC HgCdTe radiometers. The lowest responsivity uncertainty is achieved when these non-uniform radiometers are operated in irradiance measurement mode, where the incident uniform field of radiation averages out the detector's non-uniformity related uncertainties. The angular response deviation from the cosine function within the 16° FOV of the radiometers dominates the uncertainty budget for irradiance responsivity measurements in the 3 µm to 20 µm sensitivity range of these working standard devices.

## 1. Introduction

Because of their high sensitivity and fast response, mercury cadmium telluride (HgCdTe or MCT) detectors have been widely used in many advanced infrared (IR) systems. Besides military and space applications, HgCdTe detectors also find important uses in industry, medicine and research. The demands of these users have resulted in focused efforts on long wavelength infrared (LWIR) focal plane arrays (FPAs) and detectors with higher operating temperatures [1].

The spatial uniformity of the responsivity of detectors is one of the most important characteristics for applications requiring quantitative measurement. Additionally, for radiometric applications, one is often interested in the angular dependence of the responsivity in both power (underfilled) and irradiance (overfilled) modes [2]. Due to the complex crystal structure and growth processes, it is more difficult to manufacture HgCdTe materials and devices with good uniformity than simpler systems such as Si and GaAs. As a result, direct characterization of the spatial uniformity of responsivity (mapping) of HgCdTe radiometers provides essential information for both end-users and manufacturers.

The National Institute of Standards and Technology (NIST) provides spatial uniformity measurements of responsivity over the 200 nm and 1800 nm spectral range [3]. Most reports of detector spatial uniformity available in the literature are limited to the UV, visible and near IR spectral regions [4–7]. For long wavelength HgCdTe detectors, however, the results measured at short wavelengths can be significantly different from those measured at long wavelengths because the optical absorption coefficients vary considerably as a function of photon energy, especially near the absorption edge [8]. The responsivity of HgCdTe detectors also depends on the quantum efficiency, the effective minority carrier lifetime, and other parameters that vary with the optical absorption coefficient. The spatial uniformity of the responsivity of HgCdTe detectors

  

at long wavelengths has been reported by the National Physical Laboratory [9, 10] but not the angular dependence.

To investigate the performance of HgCdTe radiometers being developed for a comprehensive detector calibration facility at NIST [11], we established a capability for characterization of both spatial and angular uniformity of the responsivity of detectors at long wavelengths. In this paper, we describe an apparatus based on a 10.6 µm $CO_2$ laser for spatial and angular response uniformity measurements. The results for three HgCdTe LWIR radiometers are presented.

## 2. Apparatus set-up

The apparatus for spatial and angular uniformity of responsivity measurements consists of four parts as shown in figure 1: (1) a stabilized $CO_2$ laser source system, (2) a beam manipulation and control system, (3) a motorized detector translation–rotation system and (4) a signal processing and instrument control system.

### *2.1. Stabilized $CO_2$ laser system*

For large-area detectors and detailed spatial measurements, it is important to have a stable laser source system. A laser stabilizer with a feedback dither stabilization circuit is used for this purpose. An optical feedback detector mounted in the $CO_2$ laserhead is used to maintain a stable output power. The $CO_2$ laser has a 4 W maximum output power at the 10 P(20) line (10.59 µm) and can be grating tuned from 9.17 µm to 10.86 µm.

A temperature-controlled water cooling system is also used. As shown in figure 2, the variation of the $CO_2$ laser output power over the measurement periods of 4 h for each detector (identified in the legend) is typically within ±0.2% to ±0.3%. A reference pyroelectric detector is used to monitor the laser power. The steps in the L6296 data are not caused by laser instability but indicate momentary interruptions in the measurement process.

### *2.2. Beam control system*

The laser output beam in figure 1 passes through a spatial filter/beam expander to improve the beam collimation, uniformity and downstream imaging. A beam steerer with two adjustable flat mirrors is used to set the height and steer the beam both vertically and horizontally. A computer-controlled two-polarizer attenuator is used to reduce the laser power to a level appropriate to the detector under test. The first beam splitter transmits a portion of the light into another system for IR scatter measurements. The reflected portion passes through a second beam splitter to the monitor (reference) detector. The second reflected beam is further attenuated by neutral-density ultrathin filters with optical densities (OD) of 2, 3 and 5 before being focused onto the test detector. Through careful selection of polarizer settings as well as the filters, power levels from nanowatts to watts are available. A meniscus lens is used to focus the beam onto the test detector. It provides a sufficiently small spot for spatial mapping of the detectors under test. A 0.3 mm diameter spot is easily achievable with this apparatus for the 10.6 µm $CO_2$ laser beam. With an aspheric lens, a smaller spot size may be obtained for smaller area detector characterization.

### *2.3. Detector manipulation system*

The test detectors are mounted on a three-dimensional translation stage with motorized $X$–$Y$ and manual $Z$-axes that in turn are mounted on a motorized rotation stage. The detector surface is oriented parallel to the $X$ (horizontal)–$Y$ (vertical) plane. The $Z$-axis is parallel to the incident beam and perpendicular to the detector surface. The rotation stage is mounted onto another translation stage travelling in the

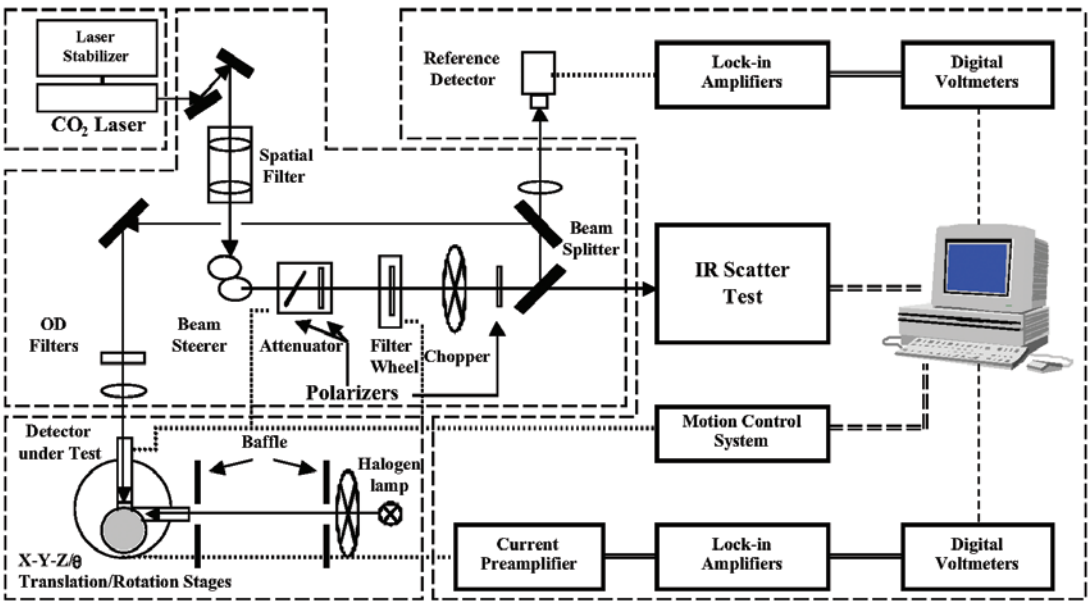


**Figure 1.** Schematic diagram of the spatial/angular uniformity of responsivity measurement set-up at 10.6 µm.

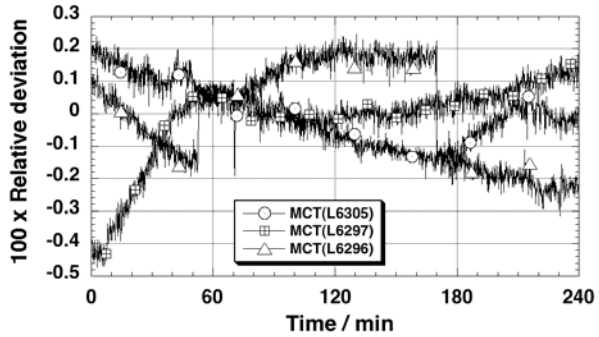


**Figure 2.** Stability of $CO_2$ laser during the spatial uniformity measurements.

$X$ direction. This second $X$ stage enables orientation of the rotation stage axis to intersect with the beam. This movement is the first step of the alignment process. The second step is to place the axis of the rotation stage in the surface plane of the detector (i.e. the $X$–$Y$ plane). The third step is to place the beam focus at the detector surface (and centre in most cases). The alignment is carried out with sufficient precision so that the input light spot remains in place as the detector is rotated for angular dependence measurements. A detailed description of this procedure is presented in section 3.2. For angular dependence measurements performed in overfilled mode, the rotation stage is mounted vertically.

### *2.4. LabVIEW control programming*

Operation of the entire measurement process is controlled through LabVIEW based programs. This includes control of motion of the detector stages for both translation and rotation, laser power attentuation through polarizer rotation, filter interchange, data acquisition by lock-in amplifiers and digital voltmeters, and data analyses and storage.

## 3. Experimental

### *3.1. Sample description*

The samples are large-area long-wavelength photoconductive (PC) HgCdTe radiometers developed in cooperation with Belov Technology, Inc.[3]. The detector elements have no cutlines in their active areas, as opposed to most conventional large area PC HgCdTe detectors that typically contain one or more cutlines. The absence of cutlines results in some reduction in sensitivity due to low detector resistance, but it removes the strong variations in the vicinty of the cutlines. The arrangement of baffling that defines the radiometer's field of view is shown in figure 3. The active area of the PC HgCdTe detector elements is 3 mm × 3 mm or 4 mm × 4 mm square. The spectral response is from 2 µm to near 20 µm. The resistance of these cutline-free detectors is 15 Ω or less. The aperture in front of the 4 mm detector is circular and 3.5 mm in diameter. No aperture is mounted in front of the 3 mm detector. The field-of-view (FOV) of 17° is determined by the second aperture in the cold baffle tube.

[3] Certain commercial products are identified in this paper. Such identification is not intended to imply recommendation or endorsement by NIST.

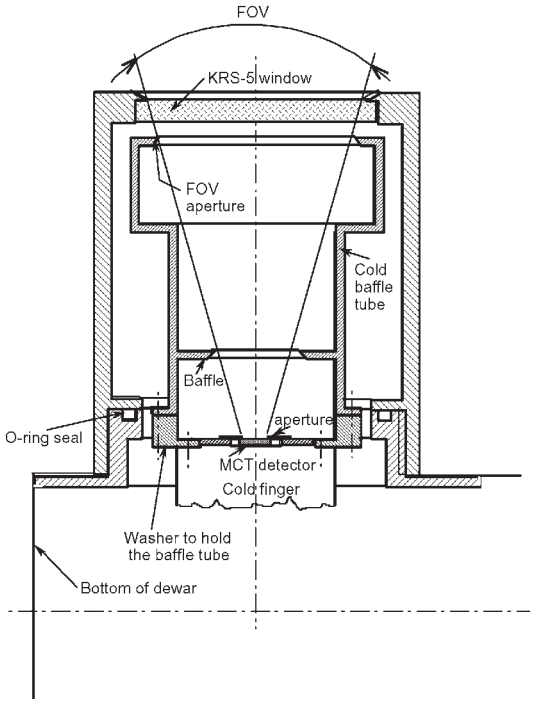


**Figure 3.** Design of the input geometry defining optics in the PC HgCdTe radiometer dewar.

### *3.2. Detector alignment procedure*

Careful alignment of the detector using all available stages is critical for obtaining accurate spatial and angular responsivity data. It requires considerable attention and patience. We present a brief description of the process. Recall that the $X$–$Y$–$Z$ stage holding the detector is mounted on top of a rotation stage.

First, scans are performed in both the $X$ and $Y$ directions to locate the edges of the detector (where the signal reaches half its magnitude at the detector's centre). Then, after centring on $Y$, the $X$ coordinate is set to an edge. Next, the rotation stage is turned a small amount (e.g. 7°). Then the $Z$-axis is adjusted manually to again reach a signal level of half magnitude. Since the input beam has been previously aligned to intersect the axis of the rotation stage (first step of the stage alignment described in section 2.3), the edge of the detector will be coincident with the axis of the rotation stage. A check on this alignment result is shown in figure 4 in the form of $X$-axis scans at +7°, 0° and −7° angles of incidence. Note the good repeatability obtained.

## 4. Results and discussion

After alignment, several sets of measurements were performed to characterize the radiometer responsivity variations. These measurements are performed both for uncertainty evaluation and for selection of the best mode of operation of the radiometers with the least associated measurement uncertainties. Here, we report results for three HgCdTe radiometers.

The spatial variation of responsivity was measured over the entire detector surface for the three radiometers. Step sizes of 0.1 mm in both directions were used. The results are

shown as contour plots of the relative responsivity for 10.6 µm radiation in figure 5.

We also measured the angular variation of power responsivity at nine locations within the 2 mm × 2 mm central region separated by 1 mm steps to assess the spatial uniformity of the angular dependence of responsivity. The coordinates for the set of nine angular dependent measurements are (in millimetres) (−1, −1), (0, −1), (1, −1), (−1, 0), (0, 0), (1, 0), (−1, 1), (0, 1) and (1, 1), which correspond to the coordinates in the spatial maps in figure 5. Results of the angular responsivity variation measurements are shown in figure 6 for all three detectors.

Measurements of the angular variation of power responsivity shown in figure 6 were made with *p*-polarized light. The polarization state should affect the angular repsonsiviity according to the Fresnel reflection equations. However, in the case of highly spatially non-uniform detectors such as the MCTs in this study, the variation may be dominated by small spatial shifts due to a minor misalignment of the detector surface and the rotation axis. Hence we would not anticipate significant differences between the results in figure 6 and those for *s*-polarized or unpolarized equivalent measurements.

For power mode measurements, where the detecting element must be underfilled, spatial non-uniformity can result in large measurement errors. For the radiance and irradiance modes, the radiometer is overfilled and the effects of spatial non-uniformity are reduced. This reduction can be seen in the results of the plots of the angular response variation in figure 7, in which the range of responsivity variation from the ideal cosine response is nearly an order of magnitude less than seen in figures 5 and 6. For these measurements, a ceramic source heated to approximately 1000 °C was used to illuminate the radiometers. Aside from some baffling to reduce spurious inter-reflections, no other intervening optics were used. The radiometer was rotated about both horizontal and vertical axes by alternating horizontal and vertical mounting of the rotation stage. To qualitatively compare the response behaviour for the broadband illumination to that for 10.6 µm light, curves of the averages over the nine (seven) points in figure 6 are also shown.

In the irradiance mode, the detector responsivity varies from the ideal cosine response in each case by an order of magnitude less than that in the power mode as shown in figure 7. Hence, we can conclude that the preferred mode of operation of these (MCT) radiometers is in the overfilled mode. Note that since the figure 6 data are for underfilled mode (no cosine dependence) operation, the corresponding average curves in figure 7 are for qualitative comparison. Nevertheless, the rough agreement of the broadband overfilled data with the analogous result at 10.6 µm of averaged angular data indicates that this is true for the radiometer's entire wavelength range.

A summary of all the results is presented in table 1. The numbers shown are the maximum deviations in the central 2 mm × 2 mm areas and within ±8° as percentages, for the spatial and angular results, respectively. The variable $f_2$ is the directional error in the overfilled mode, which is defined by [12]

$$f_2(\varepsilon, \phi) = \frac{E_r(\varepsilon, \phi)}{E_r(\varepsilon = 0^\circ)\cos\varepsilon} - 1, \tag{1}$$

where $E_r(\varepsilon, \phi)$ and $E_r(\varepsilon = 0^\circ)$ are the detector readings of the incident radiation, $E$, arriving at incident angles of $\varepsilon$ and 0°, and

$$f_{2\max} = \max\left[f_2(\varepsilon, \phi)|_{\varepsilon=-8^\circ}^{\varepsilon=+8^\circ}\right] \tag{2}$$

and

$$f_2 = \frac{1}{2}\int_{\varepsilon=-8^\circ}^{\varepsilon=+8^\circ} |f_2(\varepsilon, \phi)\sin 2\varepsilon|\,\mathrm{d}\varepsilon. \tag{3}$$

As seen in figure 5(*a*), the L6305 radiometer has the best spatial uniformity, with a level of 34%. Its angular

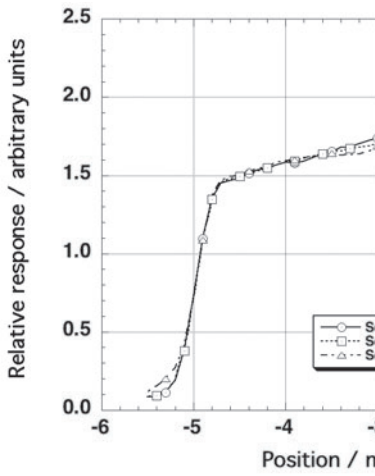


**Figure 4.** *X*-axis scan measurement results for incident angles of +7°, 0° and −7°.

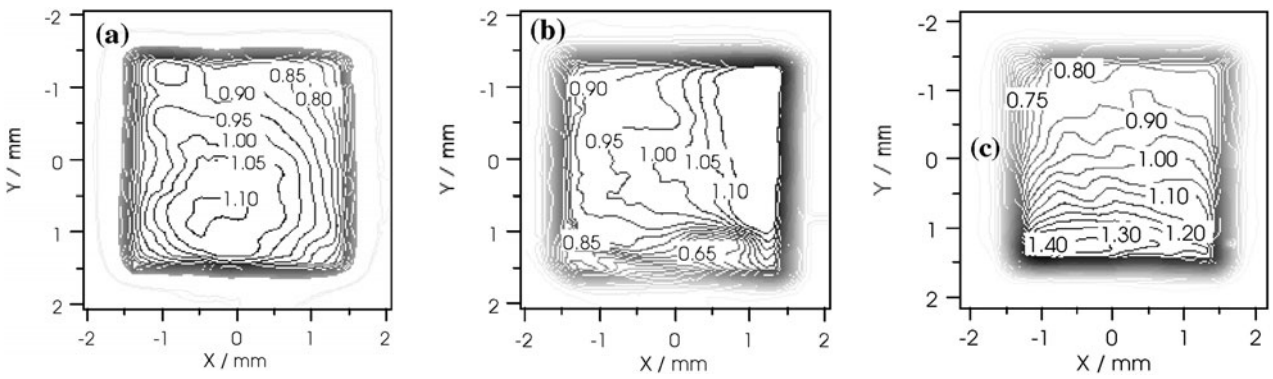


**Figure 5.** Contour plot showing the spatial variation of the relative responsivity (in arbitrary units) of three HgCdTe LWIR radiometers: (*a*) L6305, (*b*) L6296 and (*c*) L6297.

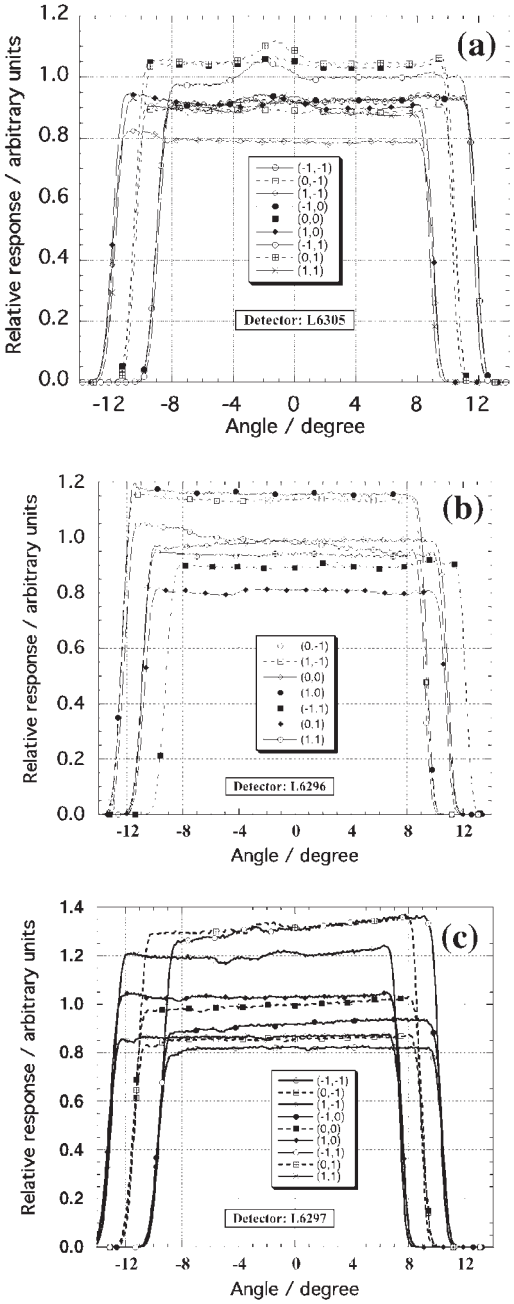


**Figure 6.** The angular variation of the relative responsivity of the three radiometers: (*a*) L6305, (*b*) L6296 and (*c*) L6297. The angular response variation was measured at nine (seven for (*b*)) locations in a 2 mm × 2 mm grid in the detector centre as indicated in the legends.

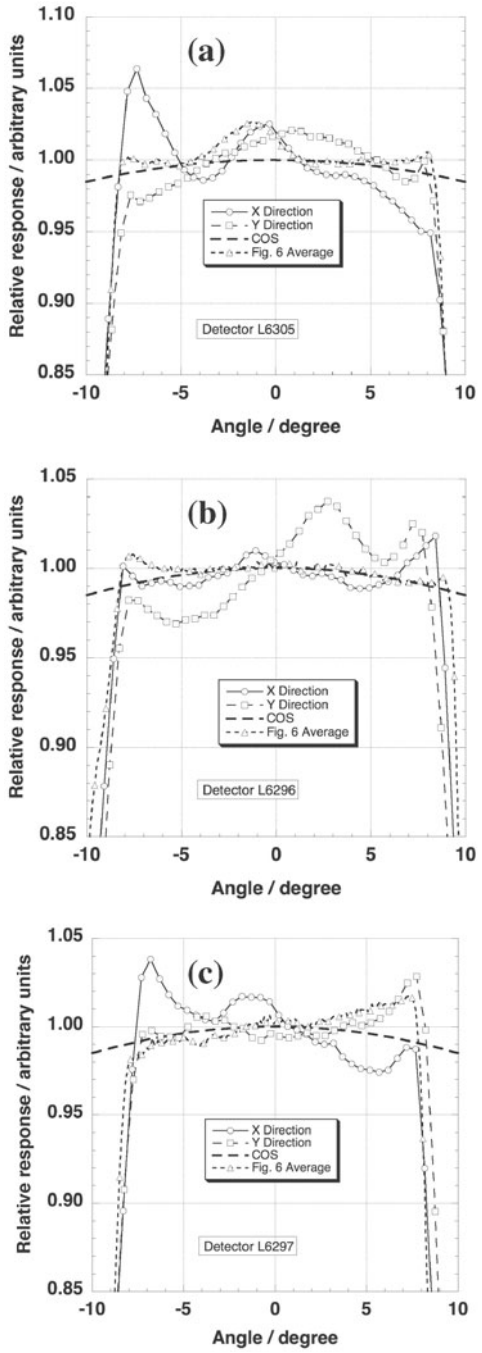


**Figure 7.** The angular variation of the irradiance mode (detector overfilled) responsivity of the three radiometers: (*a*) L6305, (*b*) L6296 and (*c*) L6297. In addition, each plot shows the ideal $\cos(\varepsilon)$ dependence as well as an average of the curves shown in the corresponding plots of figure 6.

dependence variation in the underfilled mode in figure 6(*a*) is poor at $Y = 1$ mm due to an apparent bump around $1^\circ \sim 2^\circ$ incident angles. We can also see bumps at $Y = 0$ mm that are much smaller where the variation is better. The responsivity increases slightly where the input beam hits the edges of the radiometer aperture. Its angular dependence variation in overfilled mode is similar at the level of several per cent. For the L6296 radiometer, no bumps exist and the uniformity of the angular dependence variation in the underfilled mode appears better except at (1,1). Its angular dependence in the overfilled mode is much better. For the L6297 radiometer, however, the spatial uniformity is worse, and there are some significant dips in the angular responsivity in the underfilled mode that are not obvious in the plot. These dips may be due to the window of the radiometer dewar. A window effect also exists in the spatial uniformity measurements but is less than the non-uniformity of the HgCdTe detector itself. Other measurements such as transmittance mapping of the window will help to understand the effect of the window non-uniformity on the radiometer performance. Nevertheless, end-users of the radiometers are primarily interested in the combined performance of the

**Table 1.** Compilation of the results of spatial and angular uniformity measurements: relative variation of variable × 100.

| Radiometers | Spatial in 2 × 2 | Angular in underfilled mode at nine points | | | | | | | | | $f_{2\,\max}$ | | $f_2$ | |
|---|---|---|---|---|---|---|---|---|---|---|---|---|---|---|
| | | (−1, −1) | (−1, 0) | (−1, 1) | (0, −1) | (0, 0) | (0, 1) | (1, −1) | (1, 0) | (1, 1) | *X* | *Y* | *X* | *Y* |
| L6305 | 34 | 4.4 | 4.4 | 7.8 | 2.5 | 3.7 | 8.4 | 3.7 | 4.5 | 6.7 | 6.0 | 3.8 | 6.2 | 3.8 |
| L6296 | 38 | — | — | 2.9 | 1.8 | 3.3 | 2.1 | 2.1 | 2.1 | 10.5 | 1.9 | 4.2 | 1.4 | 4.2 |
| L6297 | 53 | 1.9 | 5.2 | 8.8 | 2.2 | 5.3 | 6.2 | 1.6 | 2.1 | 5.6 | 3.6 | 4.3 | 3.5 | 2.6 |

window and detector. Considering both spatial and angular uniformity of responsivity in both the underfilled and overfilled modes, no one radiometer stands out. For selection of a single radiometer operating in the preferred overfilled mode, L6296 exhibited the best performance. For all three radiometers, the angular dependence of responsivity in the overfilled mode is consistent with that in the underfilled mode.

It should be noted that the use of appropriate aperturing of the detector can optimize performance. Often the responsivity is peaked at an edge or corner of the detector or is non-zero beyond its edge due to inter-reflections etc. The aperture can be used to eliminate these regions from exposure to the incident radiation, resulting in more uniform response. The use of baffles in combination with apertures can help to reduce inter-reflection effects.

## 5. Conclusions

We have used a stabilized $CO_2$ laser source system, a beam manipulation and control system and a motorized detector translation–rotation system, to characterize both the spatial and angular uniformity of responsivity of LWIR HgCdTe radiometers. The surface alignment of the detector is crucial for angular uniformity measurements. Three HgCdTe radiometers were measured. For each detector, the response varies across the entire surface, not just at the corners/edges where the electrode contacts are found. The results show that the best spatial uniformity within a 2 mm × 2 mm area of an element is 34%, while the angular uniformity of responsivity in both modes is significantly better. Some variability between detectors was observed. However, the general result of significantly better performance in the overfilled mode (as compared with that in the underfilled mode) is true for all detectors tested. The window of the dewar may affect the results of the angular uniformity measurements.

## References


[1] For a review of recent progress, see the special issue on the 1998 US Workshop on the Physics and Chemistry of II–VI Materials 1999 *J. Electron. Mater.* **28** 581

[2] Lehman J, Eppeldauer G, Aust J A and Racz M 1999 *Appl. Opt.* **38** 7047

[3] Larason T C and Bruce S S 1998 *Metrologia* **35** 491

[4] Gullikson E M, Korde R, Canfield L R and Vest R E 1996 *J. Electron Spectrosc. Relat. Phenom.* **80** 313

[5] Lei F and Fischer J 1993 *Metrologia* **30** 297

[6] White M G and Bittar A 1993 *Metrologia* **30** 361

[7] Stock K D, Heine R and Hofer H 1991 *Metrologia* **28** 207

[8] Pautrat J L and Magnea N 1994 *Properties of Narrow Gap Cadmium-based Compounds* EMIS Datareview Series No 10, ed P Capper (London: Inspec) p 75

[9] Fox N P, Prior T R, Theocharous E and Mekhonstsev S N 1995/96 *Metrologia* **32** 609

[10] Theocharous E, Fox N P and Prior T R 1996 *Proc. SPIE* **2815** 56

[11] Brown S W, Eppeldauer G P and Lykke K R 2000 *Metrologia* **37** 579

[12] Central Bureau of the Commission Internationale de L'Eclairage 1982 *Methods of Characterizing the Performance of Radiometers and Photometers* CIE Publications No 53 (TC-2.2) 12